

Determination of Linear Polarization and Faraday Rotation of Pulsar Signals from Spectral Intensity Modulation

P. S. Ramkumar & A. A. Deshpande, *Raman Research Institute, C.V Raman Avenue, Bangalore 560 080, India.*

Received 1999 March 19; accepted 1999 June 24

Abstract. Most of the known pulsars are sources of highly linearly polarized radiation. Faraday rotation in the intervening medium rotates the plane of the linear polarization as the signals propagate through the medium. The Rotation Measure (RM), which quantifies the amount of such rotation as a function of wavelength, is useful in studying the properties of the medium and in recovering the intrinsic polarization characteristics of the pulsar signal. Conventional methods for polarization measurements use telescopes equipped with dual orthogonally polarized feeds that allow estimation of all 4 Stokes parameters. Some telescopes (such as the Ooty Radio Telescope) that offer high sensitivity for pulsar observations may however be receptive to only a single linear polarization. In such a case, the apparent spectral intensity modulation, resulting from differential Faraday rotation of the linearly polarized signal component within the observing bandwidth, can be exploited to estimate the RM as well as to study the linear polarization properties of the source. In this paper, we present two improved procedures by which these observables can be estimated reliably from the intensity modulation over large bandwidths, particularly at low radio frequencies. We also highlight some other applications where such measurements and procedures would be useful.

Key words. Stars: neutron—pulsars—interstellar medium: Faraday rotation—telescope: polarization.

1. Introduction

Pulsar signals are generally weak (with average flux densities ranging from a few milli-Jansky to a few Jansky), with a high degree of linear polarization. The position angle of the linearly polarized component changes as a function of longitude within the pulse in a manner that depends on the geometry of the spin axis and magnetic poles of the pulsar relative to the observer's line-of-sight (Radhakrishnan & Cooke 1969). At a given longitude, the average polarization seems to have a good long-term stability in most cases, but the apparent plane of linear polarization rotates as function of frequency across the band due to Faraday rotation in the intervening medium. The extent of the rotation θ is given by

$$\theta = \text{RM} \lambda^2 \tag{1}$$

Where λ is the wavelength of observation and RM is the Rotation Measure ($= \int_0^D n_e B_{\parallel} dl$ where n_e is the electron density, B_{\parallel} is the line-of-sight component of the magnetic field and D is the distance to the source). It is clear from this equation that by measuring the polarization position angles at different frequencies spanning a sufficiently wide band one can estimate the Rotation Measure (RM). Usually, polarization measurements use antennas with dual orthogonally polarized feeds. By measuring the Stokes parameters across the spectrum or at several suitably separated frequencies, the amount of Faraday rotation is determined. At low radio frequencies, the Faraday rotation of the position angle becomes large enough to be able to measure, the differential rotation within even moderate bandwidths. In addition, the pulsar signal is generally stronger at lower frequencies, although at very low frequencies the strong galactic background radiation seriously affects the sensitivity of these measurements. Thus such measurements require a suitable observing frequency, large bandwidths and sensitive telescopes to achieve the required accuracy. The number of pulsars for which RM has been estimated is only about 260 (Taylor *et al.* 1993) out of about 1000 known pulsars. Most of these 260 pulsars are strong sources and hence relatively easy to study also for their polarization characteristics. To extend such studies to weaker pulsars and at low radio-frequencies, large telescopes operating at suitable frequencies are required. Some telescopes may have large collecting areas, but are receptive to only a single linear polarization. In such cases, an indirect way exploiting the effect of Faraday rotation can be used for studying the linear polarization properties of continuum sources. The basic principle involved in this type of measurements is outlined below.

For simplifying the following discussion, we assume that the RM contribution of the interstellar medium and the ionosphere are constant over the period of observation and consider the time-varying effects of these media later. When a 100% linearly polarized wave is incident on a linearly polarized antenna, the amount of power received by the antenna depends, among other things, on the angle ζ between the directions of polarization of the wave and the antenna feed as

$$P_{\text{received}} = \frac{P_{\text{lin}}}{2} [1 + \cos(2\zeta')] \quad (2)$$

where P_{lin} is the linearly-polarized incident power. The incident polarization position angle changes at different frequencies within the observed bandwidth due to the Faraday rotation in the medium between telescope and the source. Then, even if the power radiated by the pulsar at all frequencies remained the same, the power received by a linearly polarized antenna would show a modulation across the band as shown in Fig. 1. The sampled version of the power spectrum is given by

$$P(f_L + i\Delta f) = A_0 + A_1 \cos \left\{ 2 \left(\zeta + \left(\frac{\text{RM}c^2}{(f_L + i\Delta f)^2} \right) \right) \right\} \quad \text{for } i = 0, 1, \dots, N \quad (3)$$

where c is velocity of light, f_L is the lower edge-frequency of the spectrum, Δf is the bandwidth of each frequency channel, i is the channel number, A_0 is the average power, A_1 is the linearly polarized power, ζ is the intrinsic position angle of radiation relative to the antenna polarization angle and the second term in the argument is the total Faraday rotation ($\theta_i = \text{RM}\lambda_i^2$). The following can be determined from the modulation:

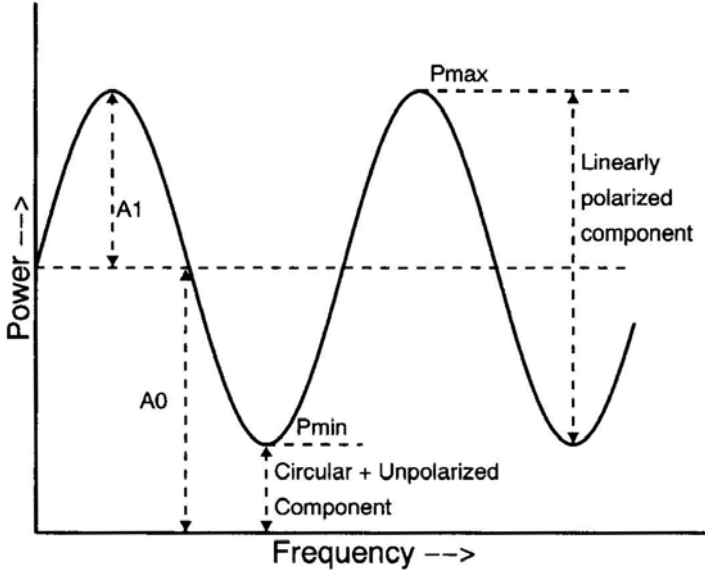


Figure 1. The modulation due to Faraday rotation in the spectrum of the power received by a single linearly polarized antenna.

- (1) The degree of linear polarization, d_1 , can be determined by simply measuring the depth of modulation, as

$$d_1 = \frac{P_{\max} - P_{\min}}{P_{\max} + P_{\min}} = \frac{(A_1)}{(A_0)} \quad (4)$$

where P_{\max} and P_{\min} are the maximum and minimum values of the apparent spectral power contribution, respectively.

- (2) By observing with a bandwidth B over which the modulation completes X_0 cycles, the Rotation Measure can be estimated as

$$\text{RM} = \frac{X_0 \pi}{c^2} \left[\frac{1}{f_L^2} - \frac{1}{(f_L + B)^2} \right]^{-1} \quad (5)$$

- (3) The phase (ϕ) of the modulation pattern (i.e. the argument of the cos term in equation (3)) depends directly on the intrinsic position angle of the radiation. Therefore, at a fixed frequency, the variation of ϕ as a function of the pulse longitude can be used to trace the intrinsic sweep of the position angle during the rotation of the pulsar. Using the ϕ value at a reference frequency, say f_L , ζ can be estimated as

$$\zeta = \frac{\phi_0}{2} - \left(\frac{\text{RM} c^2}{f_L^2} \right) \quad (6)$$

where $\phi = \phi_0$ at $f = f_L$.

- (4) Knowing the dispersion measure (DM in pc cm^{-3}) and the rotation measure (RM in rad m^{-2}), the mean line-of-sight component of the magnetic field (weighted by the electron density) can then be estimated from the relation

$$\langle B_{\parallel} \rangle = 1.235 \left[\frac{\text{RM}}{\text{DM}} \right] (\mu \text{ Gauss}). \quad (7)$$

The basic method outlined above has been used earlier (Sulemanova *et al.* 1988) for polarization measurements of 18 pulsars. However, they model the modulation phase to vary linearly with the radio frequency which does not account properly for the non-linear dependence of ϕ (see equation 3), particularly at low radio-frequencies and over large fractional bandwidths.

A modified, more direct method to estimate $\langle B_{\parallel} \rangle$ along the directions to pulsars has also been used by Smirnova & Boriakoff (1997). In this method, the data are not dedispersed and the spectral modulations translated to an equivalent temporal modulation (through the dispersion law) are monitored across the pulse longitude. This treatment exploits the similarity between the non-linear frequency dependences of Faraday rotation and dispersion making the temporal modulation phase a linear function of time. Despite the elegance and simplicity of this procedure, it unfortunately suffers from several disadvantages. The depth of the modulation decreases with large position angle sweeps across the pulse, and with smoothing by the finite pulse width. The method is not applicable for ‘continuous’ sources, and for pulsed sources it has a poorer signal-to-noise ratio than potentially available. And finally, the modelling of various effects in this work is less than satisfactory.

In this paper we explore two different approaches (which are presented in the next two sections). We also present some test observations and the results obtained using these two approaches. In the last section, we compare the two approaches and discuss their limitations and advantages.

2. Autocorrelation (ACF) domain approach

We begin by noting that it is difficult to detect weak modulation across the band directly from the power spectrum. If the modulation was a simple sinusoid (as in Fig. 1), the domain best suited for studying its parameters would be the ‘auto-correlation’ domain. In this hypothetical case, it would correspond to a narrow feature in the auto-correlation function obtained through a Fourier Transform of the power spectrum. The ‘lag’ associated with the feature would be directly proportional to the RM. The relative amplitude of the feature (with respect to the ‘zerolag’ auto-correlation) would correspond to the fractional linear polarization while the associated phase would depend on the Faraday rotation as well as on the intrinsic position angle. In the method outlined below, we exploit the simplicity of analysis in studying the modulation feature in the auto-correlation domain.

Step 1: Linearization of modulation phase: The argument of the cosine term in equation (3) has a non-linear (inverse square) dependence on the frequency of observation, and consequently on the frequency channel index in the case of a conventional spectrometer with uniform channel spacing. The spectrum can, however, be resampled in a suitable (non-uniform) manner such that the argument varies linearly with the new pseudo-frequency indices, making the modulation appear as a pure sinusoidal wave as a function of the new ordinate. This *linearization* simplifies the analysis and enables the use of linear methods, such as Fourier transforms, to detect and interpret the possible periodic feature directly in terms of the RM, ζ and % linear

polarization. The relation between the new (pseudo-frequency) channel index, j , and the original (true frequency) index i , is given by

$$j = \frac{\alpha \left(\frac{1}{(f_L + i\Delta f)^2} - \frac{1}{f_L^2} \right)}{\left(\frac{1}{(f_L + \Delta f)^2} - \frac{1}{f_L^2} \right)} \quad (8)$$

where the value of α can be chosen to match the new and the original modulation rate at a desired reference frequency (for example, $\alpha = 1$ will give a match at the lower-edge frequencies).

The range of j is that implied by the range of i . For integer values of j , the corresponding i values are not integers in general. Therefore, a suitably interpolated spectral contribution from the original spectrum is to be obtained for a given j . Alternatively, one may use all the samples in the original spectrum by stepping uniformly in i , where for each i , the spectral contribution is suitably shared by new spectral channels, j & $j + 1$. Then, the share in each of the new channels should be noted, so that the linearized data may then be normalized by the respective counts. In both cases, linear interpolation would suffice provided the phase rotation between two adjacent channels is small (say, less than a radian). It is important to note that this linearization procedure is independent of the rotation measure and depends only on the nature of the non-linearity (see equation 8).

Step 2: Fourier transformation: The ‘linearized’ spectrum at each longitude is (inverse) Fourier transformed separately to obtain the corresponding ACFs to allow a detailed estimation of the modulation parameters. The magnitude of the ACF is scanned to find the location corresponding to the modulation feature, and the corresponding frequency is used to estimate the RM using equation (5).

Step 3: Estimation of parameters: The peak magnitude of the ACF feature (corresponding to the Faraday modulation) gives the value of A_1 , while that at ‘zero lag’ (the first point in the ACF) provides an estimate of A_0 . The ratio of A_1 to A_0 yields the corresponding fractional linear polarization. An estimate of A_0 is also available directly as simply the mean power in the spectrum. Removal of this mean value from the RF power spectrum before computing the ACF can significantly reduce the side-lobe leakage of the ‘zero-lag’ component in to the modulation feature. This is useful particularly when the differential Faraday rotation across the band is not large. The modulation phase ϕ_0 , is the phase at the peak of the ACF. Then, from equation (6), the intrinsic position angle ζ is estimated at different longitudes. The longitude corresponding to the centroid of the pulse in the A_0 profile is taken as a reference longitude. The final results include the fractional polarization and position angle as functions of the longitude. The uncertainty in estimates of the parameters A_0 and A_1 is given by the rms value of noise in the ACF excluding the two discrete features. When the signal-to-noise ratio (SNR) is large, the formal statistical uncertainty in the modulation feature phase (expressed in radians) is simply the reciprocal of the SNR at the peak of the modulation feature in the ACF. However, a given phase value can result from a wide range of combinations of RM and ζ values, making it difficult to decouple the uncertainties in the two. If the value of ζ is known *a priori*, then the RM estimate can be refined using the observed phase information, provided

the possible 2π ambiguity is resolved. Otherwise, only the modulation ‘frequency’ (rather than the modulation ‘phase’) can be used to estimate the RM as mentioned above. The uncertainty in RM estimated in this manner can be related to the signal-to-noise ratio as shown below.

Effect of nonintegral number of modulation cycles: If the number of modulation cycles within the bandwidth is not an integer, then the modulation feature contribution will not be centered on one of the sampled points in ACF with nominal delay resolution ($1/B$). This is generally the case, necessitating finer sampling of the ACF to avoid appreciable additional errors in the estimation of the location and other parameters of the ACF feature. The required over-sampling is achieved by artificially extending the spectral span by suitably zero-padding the trailing edge of the measured spectrum or by a direct sinc-interpolation of the ACF. The SNR of the ACF feature dictates the optimum over-sampling factor and in turn implies the uncertainty in the RM estimation. It is easy to see that the uncertainty σ_x in estimation of the location x_0 of the feature is given by $\text{sinc}(\sigma_x) = (1 - 1/\text{SNR})$ where x is in units of the nominal delay-resolution (i.e. $1/B$). Also, the optimum over-sampling factor is then simply $\sim 1/\sigma_x$. From the estimates of x_0 and σ_x the RM and the corresponding uncertainty can be estimated as

$$\text{RM} \pm \sigma_{\text{RM}} = \frac{\pi}{c^2} \left[\frac{1}{f_L^2} - \frac{1}{(f_L + B)^2} \right]^{-1} (x_0 \pm \sigma_x). \quad (9)$$

An improved RM estimation is possible by using a suitably weighted sum of the ACFs (magnitudes) across the longitude range of the pulse.

Effect of scintillation: The intensity scintillations produced due to the interstellar medium result in superposed random modulations in the RF power spectra, on the scale of the associated decorrelation bandwidth. Correspondingly, the Faraday modulation feature in the ACF is convolved with a ‘scintillation ACF feature’, resulting in reduction of the contrast of the feature of interest and thereby increasing the uncertainty in the RM estimate. This effect is expected to be small for data averaged over spans much longer than the decorrelation time-scales of the scintillations or when the decorrelation bandwidth is much wider than the width of the band observed.

3. NonLinear LeastSquare (NLS) fitting approach

In this approach, an equivalent least-squares fit solution is sought through ‘matched filtering’ and the best fit values of A_0 , A_1 , ζ and RM are obtained. In doing so, we will restrict the ‘grid’ search to RM only, and use a simple procedure to estimate (rather solve for) the other three parameters, for each of the RM values. Thus, for each of the trial RM value, a model spectrum is obtained and compared with observation and the RM corresponding to the best match is sought. For the purpose of the following discussion, we rewrite the equation (3) for the model spectrum, P_m , as

$$P_m = A_0 + A_1 [\cos(h) \cos(2\zeta) - \sin(h) \sin(2\zeta)] = \sum_{j=1}^3 C_j B_j \quad (10)$$

where B_j and C_j are the three basis functions and the corresponding coefficients respectively, and the observed pattern as $P_{\text{obs}} = P_m + n$, n being the random noise term. Here, the coefficients, $C_1 = A_0$; $C_2 = A_1 \cos(2\zeta)$ and $C_3 = -A_1 \sin(2\zeta)$, contain the parameters we wish to solve for. The basis functions, namely, $B_1 = 1$; $B_2 = \cos(h)$ and $B_3 = \sin(h)$, can be assumed to be mutually orthogonal functions in principle, except when $\text{RM} = 0$. This orthogonality can be exploited to estimate the coefficients by matched filtering (cross-correlating the P_{obs} , the observed spectral pattern, with the corresponding basis functions). Assuming that we have sampled versions of the relevant patterns/functions, the cross-correlation will estimate some measures, say X_i , such that

$$X_i = \frac{1}{N} \sum_{k=1}^N P_{\text{obs}} B_i = \sum_{j=1}^3 C_j Y_{ij} \quad \text{for } (i, j = 1, 2, 3). \quad (11)$$

Where Y_{ij} is the cross-correlation between the basis function B_i & B_j computed over the N sampled points and is formally defined as $Y_{ij} = \frac{1}{N} \sum_{k=1}^N B_i B_j$. It is easy to see that $Y_{ij} = Y_{ji}$ and ideally, $Y_{ij} = 0$ when $i \neq j$ as a result of orthogonality. In practice, however, given the available span and the sampling of the basis functions, $Y_{ij} = 0$ are non-zero even when $i \neq j$. This is no different from the ‘side-lobe leakage’ that one refers to in Fourier transforms, for example. However, given the basis functions in h for an assumed RM (and hence Y_{ij}), the coefficients C_i can be solved for in a straight forward way from the above set of equations for X_i . Note that the same formulation would result from conditions for minimization of mean square deviations (of P_m from P_{obs}) with respect to the parameters A_0 , A_1 and ζ .

Using these parameter values, a model spectrum is computed and its mean square deviation e^2 from the observed data is obtained. This procedure is repeated for several trial values of RM in fine enough steps. The best estimate of RM and the other 3 parameters corresponds to the fit with minimum e^2 . The e^2 value depends on the correctness of the model, as well as on the other sources of uncertainty in the observed pattern as already discussed. The variation of e^2 as a function of changes in the model-parameters (such as RM , A_0 , etc.) can be used to estimate the uncertainty in the parameter values. The minimum detectable change in e^2 , i.e. $\Delta_e^2 \cong e^2/N_{\text{dof}}$ can be attributed to the uncertainties in the parameter values which can be derived. In the present case, the degrees of freedom (N_{dof}) are equal to $N - 4$. The minimum detectable change in the mean-square-error can be expressed in terms of the variance associated with the estimation of individual parameters, to the first order, as

$$\overline{\Delta_e^2} = \frac{1}{N} \sum_{k=1}^N \left[\left(\frac{\partial P_m}{\partial A_0} \right)^2 \cdot \Delta_{A_0}^2 + \left(\frac{\partial P_m}{\partial A_1} \right)^2 \cdot \Delta_{A_1}^2 + \left(\frac{\partial P_m}{\partial \text{RM}} \right)^2 \cdot \Delta_{\text{RM}}^2 + \left(\frac{\partial P_m}{\partial \zeta} \right)^2 \cdot \Delta_{\zeta}^2 \right]. \quad (12)$$

Ideally, the covariances of the parameters should also be considered (e.g., for the pair RM and ζ), but are ignored here for the sake of simplicity. The entire error on the left-hand side may be associated to one parameter at a time, to get the worst-case formal statistical uncertainty in that parameter. Also, the noise statistics are assumed to be same for all the frequency channels as is usually the case. The estimation of uncertainty in RM does not include the effect of the error in ζ and assumes that there is no ambiguity in the modulation phase in multiples of 2π . In such a case, the maximum error in RM (corresponding to a phase error of $\pm\pi$) is (π^2/f_L^2)

The method outlined above is extended in a straight-forward way to a combined fit over data for a range of pulse longitudes, the only common parameter being the RM.

4. Tests and Results

The processing methods discussed above were tested first using simulated data and then applied to data from pulsar observations. As a first trial, the data on PSR 0740-28, a pulsar with reasonably large RM ($\cong 150 \text{ rad m}^{-2}$) and pulse strength ($S \cong 300 \text{ mJy}$), were obtained using the Ooty Radio Telescope with the pulsar search preprocessor (Ramkumar *et al.* 1994). The spectral data for ~ 10 minutes (sampled every 0.5 msec) from 256 frequency channels covering a band of 8 MHz (around 327 MHz) were used. For each of the spectral channels, only the deviations from their long term mean power were recorded after 1-bit quantization. The data were aligned by correcting for the dispersion delay gradient across the band, and folded over the pulsar period to improve the signal-to-noise ratio. The folded profiles of all channels were arranged in the form of a time-frequency matrix. Fig. 2 displays a 3-D plot of intensity as a function of frequency and pulse longitude. The spectral channel gain calibration was done using estimates of off-pulse rms deviations. The data were then analyzed using the ACF method. Fig. 3 shows the position angle, total (solid line) and linearly polarized intensity (dashed line) as a function of the pulse longitude. For comparison, Fig. 3(c) displays the observation at 631 MHz by McCulloch *et al.* (1978), made with the 64-m telescope at Parkes, Australia. Comparison of the modulation pattern observed on three consecutive days (at the longitude of the peak of the pulse)

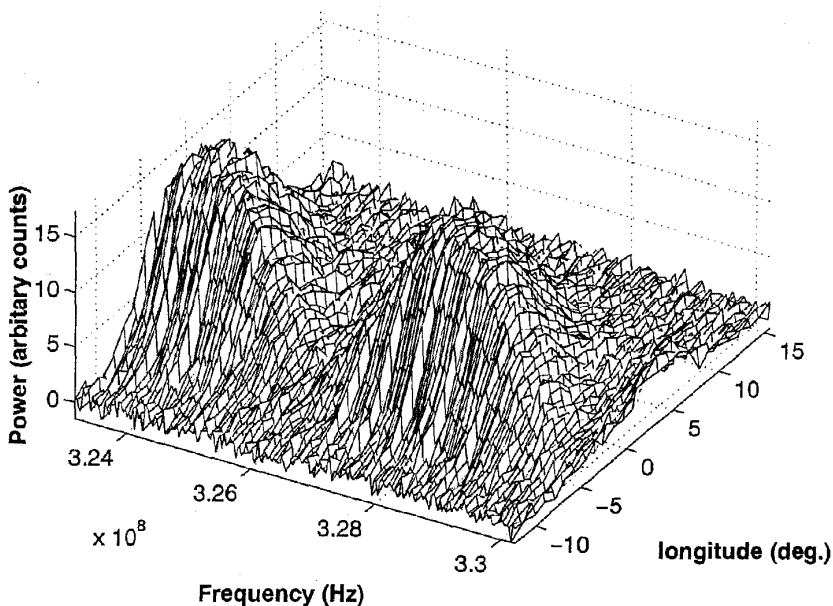
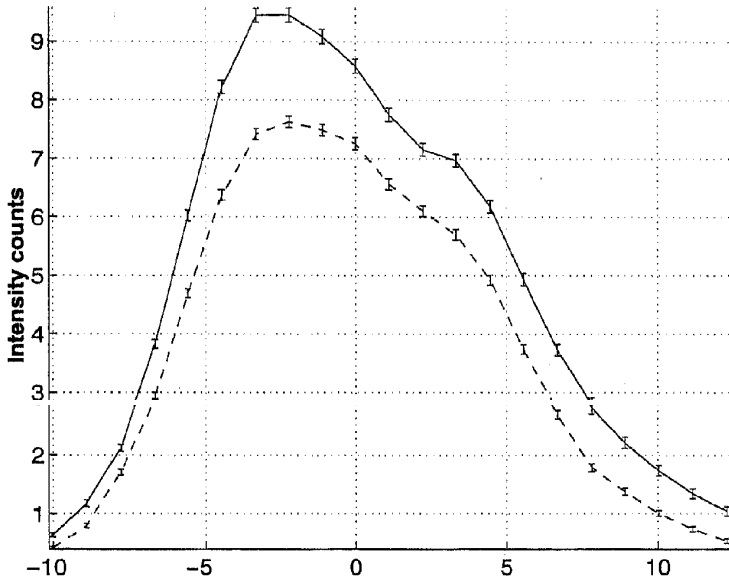


Figure 2. Pulse intensity as a function of frequency and longitude (relative to the pulse centroid) for PSR 0740-28, observed on 19-03-94 at ORT using the Pulsar Search Preprocessor.

indicates an apparent change in RM of about 0.5 rad/m^2 from day to day (shown in Fig. (4)). The rate of change is too fast to be associated with the contribution of the interstellar medium, and is more likely to be due to changes in the RM of the ionosphere. This method and initial results were discussed by Ramkumar & Deshpande (1994).

The tests were repeated on data from subsequent observations of the same pulsar using both the ACF and NLS procedures. The results from the two methods are compared in Fig. 5, where Fig. 5(a) shows the average A_0 components estimated by



(b)

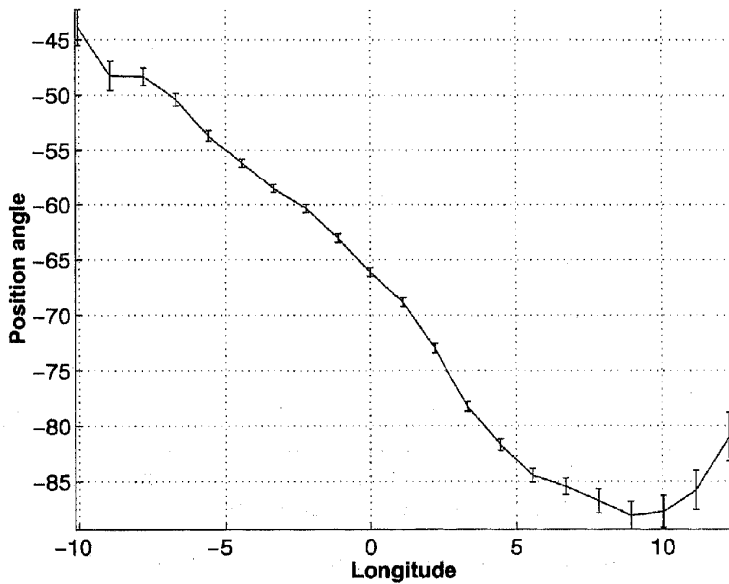


Figure 3. (Continued)

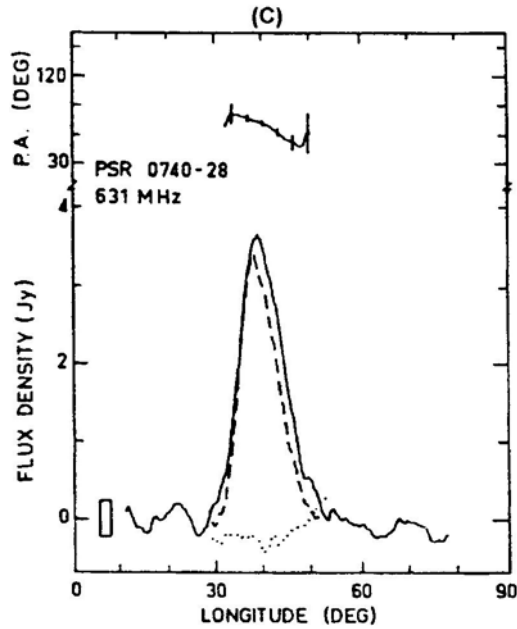


Figure 3(a,b&c). The estimated Position Angle (a) and Intensity (b) profiles of pulsar PSR 0740-28 from the observations on 19-03-94. Panel (c) shows the corresponding profiles at 631 MHz obtained by McCulloch *et al.* (1978) using dual-polarization data.

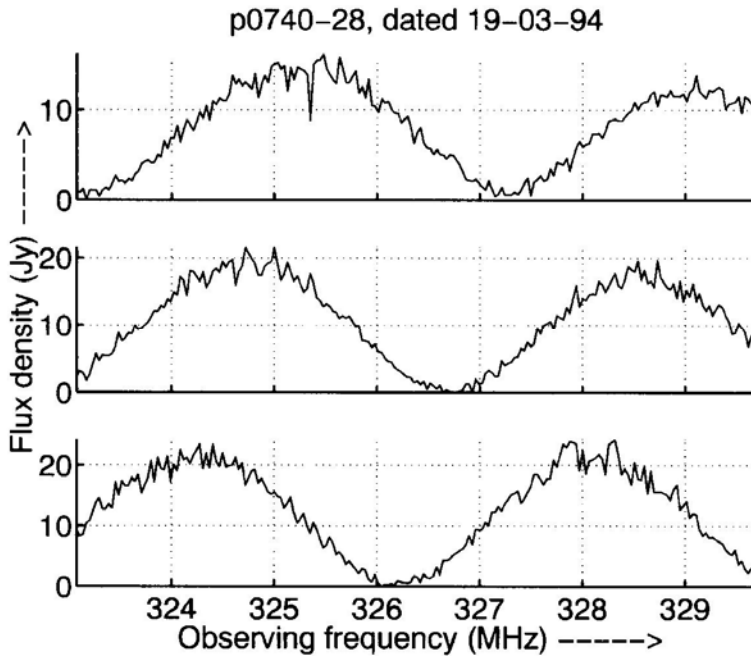


Figure 4. Average power spectra showing modulations due to Faraday rotation observed on three consecutive days (corresponding to the same nominal reference longitude). The observed differences in the modulation phase are possibly due to ionospheric RM changes.

the two methods, Fig. 5(b, c) show the corresponding fractional linear polarization d_L , and the position angle patterns respectively. The estimated value of RM (which also includes the ionosphere contribution) is 152.5 rad/m^2 and 153.5 rad/m^2 (with corresponding statistical uncertainties of 0.007 and 4.35) in the NLS and ACF methods, respectively, as compared to 152 rad/m^2 (excluding the ionospheric contribution) quoted by Hamilton & Lyne (1987).

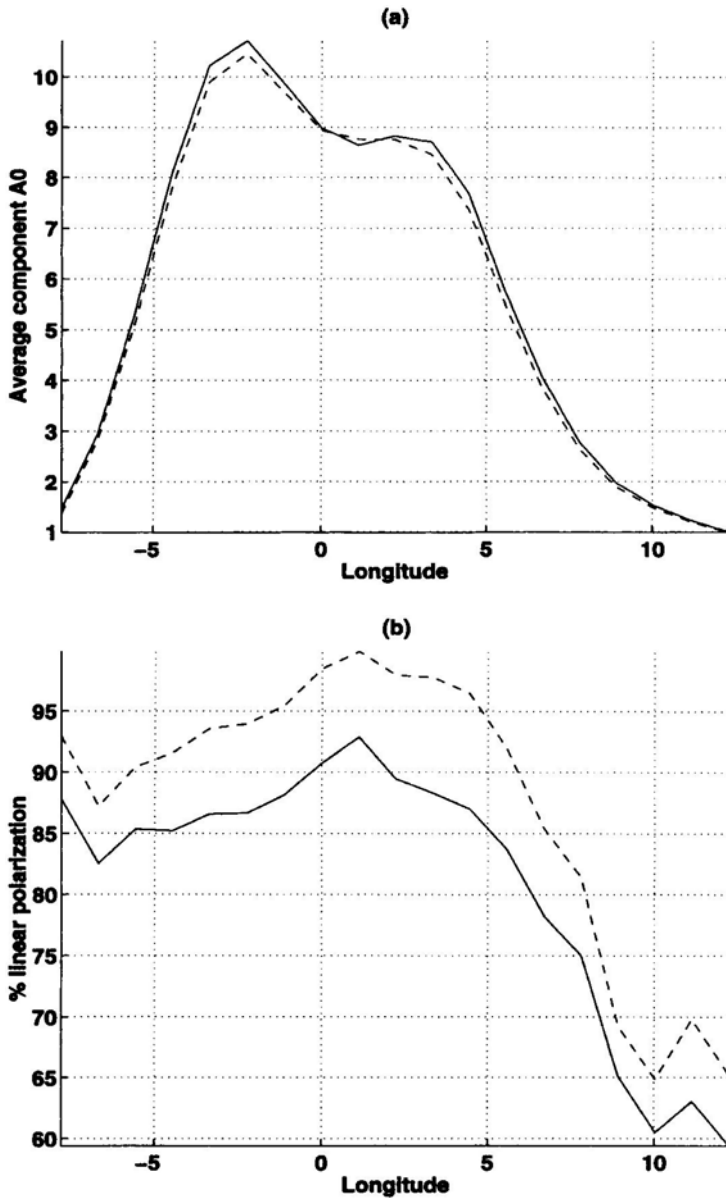


Figure 5. (Continued)

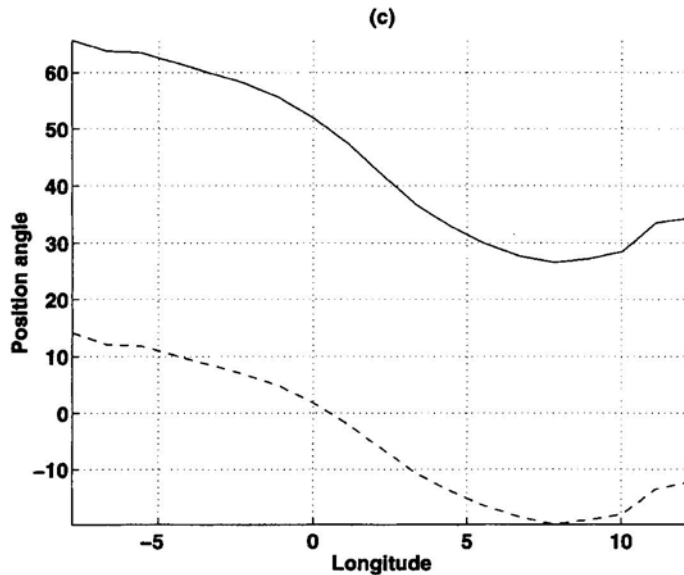


Figure 5 (a,b&c). Profiles corresponding to the best-fit parameters from the two estimation procedures applied to the data of PSR 0740-28 (observed on 15-7-1997). The solid and the dashed lines show the results from the NLS and the ACF methods respectively.

5. Discussion

In the RM determination using the basic method described here, the bandwidth and the number of spectral channels set limits to the range for measurable RM at a given operating frequency. The RM should be large enough to produce at least one cycle of intensity modulation across the band, while it should be less than a value at which one cycle of modulation spans only two frequency channels. In the ACF method, the accuracy in estimation of the parameters is also limited by the fact that “linear” interpolation was used in sharing the power of original samples to those in the linearized domain. This limits the modulation frequency that can be resampled properly, and thereby implies an upper limit for RM up to which good estimation can be made given the bandwidth, operating frequency and SNR. However, a higher order interpolation would greatly reduce this problem. In the second method, there is no such restriction since the pattern non-linearity is implicit and hence the performance is robust. As such, these methods are well suited for observations of high RM pulsars or observations over relatively large bandwidths, where simple sinusoidal approximations to modulation phase may lead to significant errors in the estimation of RM. The ACF method does not need any initial guess of RM, while the NLS method is based on a grid search over a range of RM values. In practice, it may be better to initially use the auto-correlation domain processing to arrive at an estimate of RM, and then use the non-linear fit method to refine the estimate. This approach will save the number of computations substantially, for measurements demanding high accuracy.

The ultimate uncertainty limit for RM and linear polarization measurements is set by the signal-to-noise ratio of the data particularly that of the linearly polarized

component. In the ACF method, the SNR can be enhanced further by averaging the magnitude squares of the ACFs at different longitudes thus ignoring the phase differences and using appropriate weights based on the pulse shape. The pulse longitude resolution can be suitably optimized based on the sweep rate of polarization angle within the pulse. Also, the data time span should be short compared to the typical time scales for apparent changes in the RM contributed by the ionosphere, so as to keep the depolarization due to integration well below that implied by the required RM accuracy. However, to smooth-out the undesirable modulation due to interstellar scintillations, it is desirable to average data over spans much longer than the de-correlation time scales of scintillation.

The observed modulation phase, as already noted, can be attributed to a range of combinations of ζ and RM values. The ability to *distinguish* between relative contributions from RM and ζ terms improves as the bandwidth increases or operating frequency decreases, reducing the range of degenerate combinations of ζ and RM. Since the estimated value of RM is a “weak” function of the reference modulation phase, the estimation accuracy is intrinsically higher for RM measurements compared to those of ζ . The estimation of the intrinsic position angle of the radiation can show large changes due to even a small change in the RM estimate. On the other hand, the estimation accuracy of RM and ζ is much higher in differential measurements, where any ‘changes’ in the modulation phase are interpreted as changes in only one of the two parameters (i.e. RM or ζ). Thus, the sweep of intrinsic position angle across the pulse (where RM is assumed constant) and the possible variation in RM with time (where the source position angle is constant, a fair assumption in most cases) can both be measured with high accuracy. For a given signal-to-noise ratio, the non-linear least-squares fit method has better performance than the ACF method. This is because the former method uses the complete information (amplitude and phase) of the signal to fit for RM, while in the ACF method only the amplitude information is used for the RM determination.

A comparative analysis of such observations made on a given suitable pulsar on short time spans should provide useful information about any ionospheric RM change as a function of hour-angle and time in general. As such changes are expected to be small, they would be noticeable first in the variation of the reference phase of the modulation. This information should help us in modelling the changes in the ionospheric RM reliably. The basic technique and the estimation procedures, discussed here in the context of pulsars, are also applicable to continuum sources that do not have pulsed radiation.

The ‘linearization’ technique suggested in the context of the ACF method has very useful applications in many other situations. For example, this linearization approach when applied to pulsar search data over wide bandwidths, would allow the use of Taylor’s dedispersion algorithm meant for linear dispersion delay gradients.

Acknowledgements

We thank V. Radhakrishnan for fruitful discussions and his many useful comments on the manuscript. We are also thankful to K. Kishan Rao for useful discussions and for providing support during visits by one of us (PSR) to the Regional Engineering College, Warangal.

References

- Hamilton, P. A., Lyne, A. 1987, *Mon. Not. R. Astr. Soc.*, **224**, 1023.
- McCulloch, P. M., Hamilton, P. A., Manchester, R. N., Abies, J. G. 1978, *Mon. Not. R. Astr. Soc.*, **183**, 645.
- Radhakrishnan, V., Cooke, D. J., 1969, *Astrophys. J. Lett.*, **3**, 225.
- Ramkumar, P. S., Prabu, T., Madhu Girimaji, Markendeyulu, G. 1994, *J. Astrophys. Astr.*, **15**, 343.
- Ramkumar, P. S., Deshpande, A. A. 1994, Proc. of the 16th meeting of Astronomical Society of India, Pune 1995, (ed.) V. K. Kapahi, *Bull. Astr. Soc. India*, **23(4)**, 475.
- Smirnova, T. V., Boriakoff, V. 1997, *Astr. Astrophys.*, **321**, 305.
- Suleimanova, S. A., Volodin, Yu. V., Shitov, Yu. P. 1988, *Sov. Astron.*, **32(2)**, 177.
- Taylor, J. H., Manchester, R. N., Lyne, A. G. 1993, *Astrophys. J. Suppl. Ser.*, **88**, 529.